CONF-960163--1

LA-UR- 95-4482

Title: CO_2 dial transmitter/receiver noise characterization and related correlated noise issues

Author(s): Bradly Cooke
Mark Schmitt
Roy Goeller
Steve Czuchlewski
Kenneth Fuller
Nicholas Olivas
Bryan Laubscher
Robert Sander

Submitted to: SPIE-The International Society for Optical Engineering

P.O. Box 10
Bellingham, WA 98225

Photonics West '96
#2702 Gas and Chemical Lasers

Los Alamos
NATIONAL LABORATORY

Form No. 836 R5
ST 2629 10/91

CO_2 DIAL Transmitter/Receiver Noise Characterization and Related Correlated Noise Issues

Brad Cooke, Mark Schmitt, Roy Goeller, Steve Czuchlewski, Ken Fuller, Nick Olivas, Bryan Laubscher, and Robert Sander

Los Alamos National Laboratory
MS - D448, P.O. Box 1663, Los Alamos, New Mexico 87545

ABSTRACT

Our approach concerning the development of hard target returnCO_2 DIAL transmitter/receiver systems is two phased: i) through analysis and experiment, develop a fundamental understanding of the transmitter/receiver physics specific to DIAL systems and ii) apply these fundamentals in the development of optimal performance DIAL transmitter/receiver systems.

We present our progress and results towards these objectives with the following topics addressed: A general overview of the DIAL transmitter/receiver system characterization effort with a focus on transceiver noise processes. The effects of correlated noise on DIAL performance, especially those effecting statistical convergence over long sample structures, is introduced. And, preliminary measurements of a low-noise, "white" receiver prototype are presented.

Keywords: .....CO_2 DIAL, Correlated Noise, White Transceiver System

1. INTRODUCTION: DIAL SYSTEM NOISE CHARACTERIZATION

A simplified Differential Absorption LIDAR/LADAR (DIAL) system signal chain is shown in **Figure 1**. In its simplified form, the system is composed of a laser transmitter, atmospheric transmission, target interaction, and receiver (collection optics, detection and signal processing). The basic measurement performed in DIAL is a measure of the amplitude of the hard target returned laser power/energy at a given laser line. The logarithmic difference of two or more lines provides the differential absorption information. An indication of the effectiveness of an amplitude measurement on single or multiple returns is the signal-to-noise ratio (SNR). Referring to **Figure 1**, the SNR of "*Signal*", for a DIAL measurement, is a temporal/spatial/spectral function which includes the return laser's intensity strength and fluctuations, background radiation noise, detection noise and systematic noise/error and is written as[1]

$$SNR = \sqrt{\frac{\left\langle |Signal|^2 \right\rangle}{\sigma^2_{Signal}}} \quad \text{[A/A or V/V]},$$

where $\left\langle |Signal|^2 \right\rangle$ is the mean squared signal value and σ^2_{Signal} is the signal variance. Several catagories

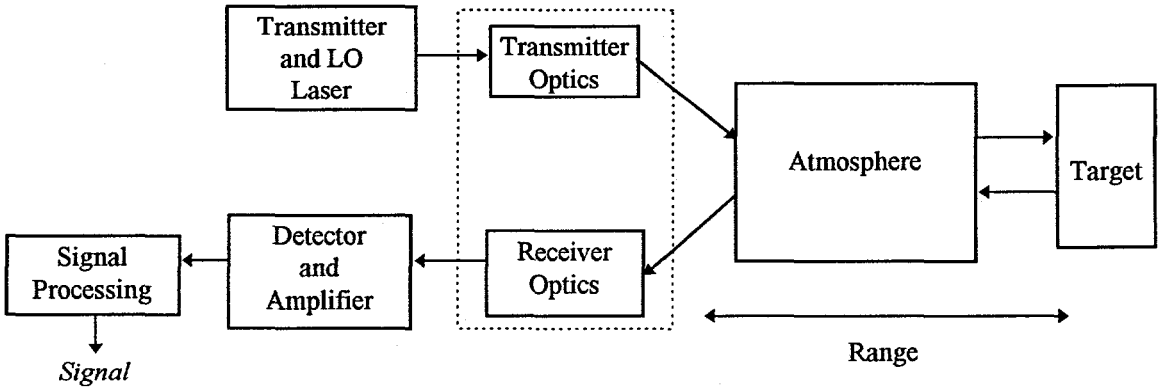

Figure 1. Simplified DIAL System Signal Chain.

can be defined:

$$SNR = \frac{\langle Signal \rangle}{\sqrt{\sigma_{\det}^2 + \sigma_{sig}^2 + \sigma_{sys}^2 \pm \rho_{c_1} \pm \rho_{c_2} \pm ..}} = \sqrt{\frac{1}{\frac{1}{SNR_{\det}^2} + \frac{1}{SNR_{sig}^2} + \frac{1}{SNR_{sys}^2} \pm \rho_{c_1} \pm \rho_{c_2} \pm ..}} \quad \text{[A/A or V/V]}$$

with:

$$SNR_{\det} = \frac{Mean\ Signal}{Detection\ Noise},$$

$$SNR_{sig} = \frac{Mean\ Signal}{Signal\ Fluctuations},$$

$$SNR_{sys} == \frac{1}{Normalized\ Systematic\ Noise \& Error},$$

$$\rho_c = Correlations.$$

The three noise categories mentioned above (SNR_{det}, SNR_{sig} , SNR_{sys}) represent the simplest statistical partitioning of most of the dominant DIAL noise/error terms currently identified. SNR_{det} is the ratio of the mean detected signal to detection noise produced by photonic noise (e.g. signal, background and coldshield shot noise) and detector/electronic noise (device dark current, impedance, amplifier/read-out and digitization noise). SNR_{sig} is a measure of the signal fluctuations (excluding detection noise) due to factors, such as, source fluctuations (transmitter laser), coherence fluctuations (scintillation, local oscillator laser), atmospheric propagation (turbulence, scatter, absorption) and target interaction (speckle, glint and albedo). SNR_{sys} accounts for systematic error sources, including hardware non-uniformities and non-linearities, optical resolution, data processing /algorithmic errors, calibration errors, and system drift. Correlations (ρ_c) occur when statistical processes are not independent. Exactly how the noise components (SNR_{det}, SNR_{sig} , SNR_{sys}) are suppressed or enhanced will depend on the application requirements and corresponding techniques and algorithms considered.

Section 2 of this paper discusses transmitter characterization with emphasis on the effects of laser fluctuations. Receiver noise and imaging efficiency is presented in **Section 3**. **Section 4** introduces preliminary work on the effects of correlated noise in DIAL systems. Finally, **Section 5** presents a prototype low-noise, white receiver detection system.

2. TRANSMITTER CHARACTERIZATION

The parameters we are most concerned with are those that characterize the average temporal, spectral and spatial beam profile and transmitted energy, and the temporal, spectral and spatial fluctuations of the beam profile and transmitted energy on a shot-to-shot basis. **Figure 2** illustrates the external (observable) parameters of interest. The transmitter aperture and beam divergence, D_x, and θ, the laser center wavelength, λ_o, and the pulse width and pulse energy τ_1, τ_2,and E_o. A brief summary of the effects (on DIAL) of the temporal, spectral and spatial fluctuations follows.

Temporal/amplitude fluctuations ($\Delta\tau_1$, $\Delta\tau_2$, Δe_o):

Fluctuations in the "start" of the transmitter pulse, $\tau_1 \pm \Delta\tau_1$, the "end" of the pulse, $\tau_2 \pm \Delta\tau_2$, and power, $P(t) \pm \Delta P(t)$, can lead to uncertainties (ΔE_o) in the transmitted energy and, hence, to uncertainties in received energy due to normalization error. In addition, the temporal fluctuations $\tau_1 \pm \Delta\tau_1$ and $\tau_2 \pm \Delta\tau_2$ can introduce detection errors in gated receivers.

A transmitter system that accurately provides a shot-to-shot measurement of τ_1, τ_2, and E_o should minimize most of the errors caused by temporal/amplitude fluctuations.

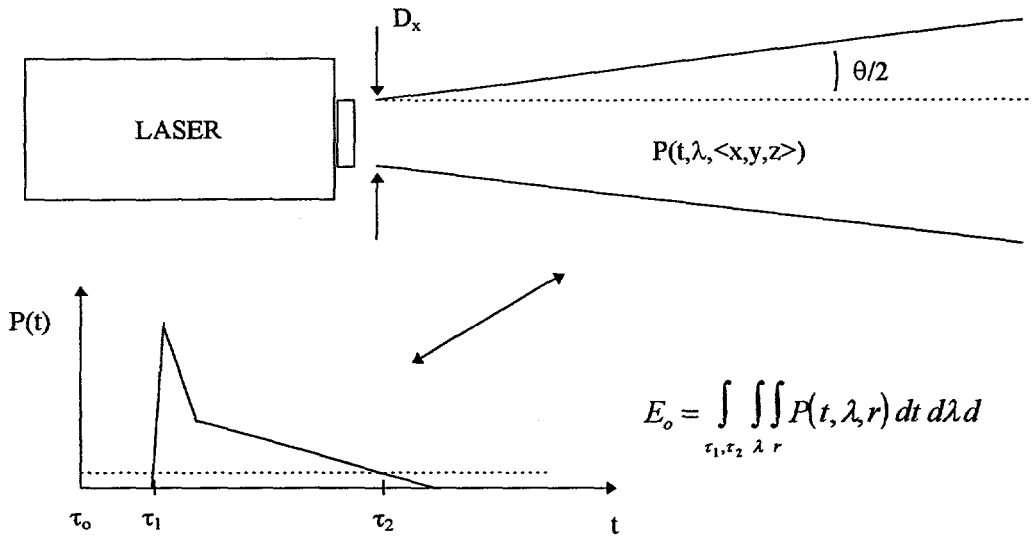

Figure 2. Laser Transmitter With Temporal Waveform.

Spectral fluctuations ($\Delta\lambda$):

Errors in measured returns can occur if drifts in the laser spectrum coincidentally overlap the edge of an atmospheric, target species or ground albedo absorption peak. Wander in the laser spectrum manifests itself as a form of correlated noise through intensity modulation at the detector. The problem is aggravated by long propagation paths.

Spatial fluctuations (Δr, Modal):

The interaction of internal transmitter optical components and laser mode/spatial fluctuations can lead to possible beam energy modulation (and beam wander). If spatial modulation is a problem, measuring the beam energy after the beam exits the transmitter optics should be considered (this seems to be easier said then done).

A useful quantity in DIAL analysis is the pulse equivalent power

$$P_{p\_eq} = \frac{1}{\tau_2 - \tau_1} \cdot \int_{\tau_1}^{\tau_2} P(t)\, dt,$$

were $P(t)$ is the temporal component of the transmitter power in **Figure 2**. The energy in the pulse is then given by

$$E_{p\_eq} = P_{p\_eq} \cdot (\tau_2 - \tau_1) = P_{p\_eq} \cdot \tau_x .$$

3. RECEIVER CHARACTERIZATION

The analysis, schematically diagrammed in Figure 3, divides the problem into two parts: i) signal detection and noise extraction and ii) imaging efficiency. Imaging efficiency quantifies the fractional optical transport efficiency from target to detector while signal detection evaluates detection efficiency in the presence of noise referenced at the detector. The two components are recombined to generate the various figures of merit required for noise studies. Section 3.1 will deal with signal detection and noise, while imaging efficiency is addressed in section 3.2.

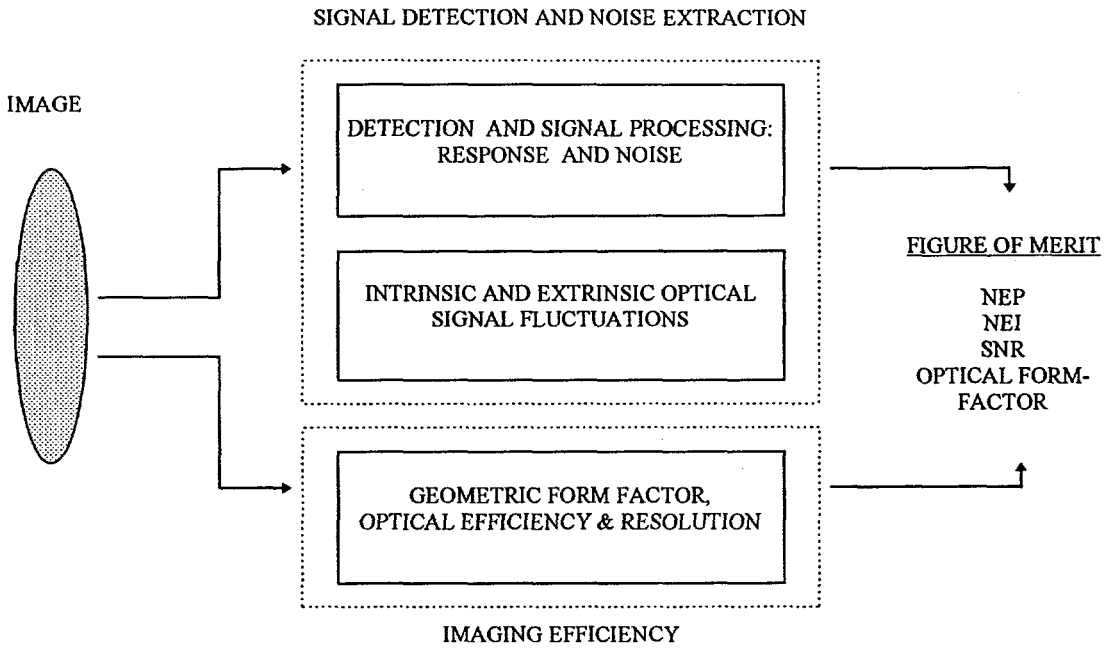

Figure 3. Analysis Approach.

3.1. Receiver noise characterization (SNR_{det})

3.1.A. Detection noise

For constant irradiance, the receiver detection signal-to-noise ratio *referenced at the detector*[2] is

$$SNR_{det} = \frac{I_{sig}}{NEI_{tot}} \qquad \text{[A/A or V/V]},$$

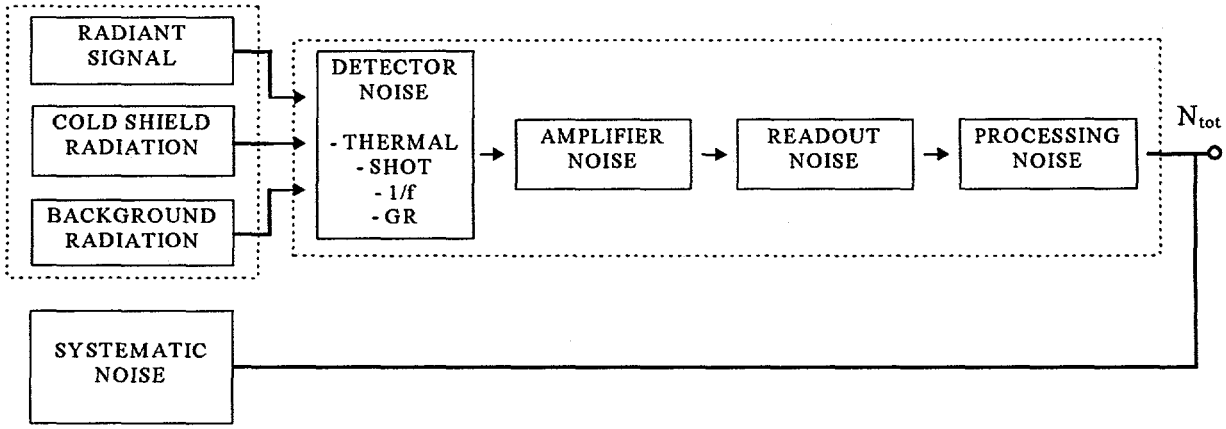

Figure 4. Detection Noise/Signal Chain.

where I_{sig} is the mean signal irradiance [ph/m^2-s] and NEI_{tot} is the total noise equivalent irradiance [ph/m^2-s]. NEI_{tot} is currently composed of three components (see **Figure 4**): photonic, detector/amplifier/readout, and a systematic term

$$NEI_{tot} = \sqrt{NEI_{ph}^2 + NEI_{dar}^2 + NEI_{sys}^2} \qquad \text{[ph/m}^2\text{-s]},$$

where:

$$NEI_{ph}^2 = NEI_{sig}^2 + NEI_{bkg}^2 + NEI_{cs}^2 \qquad \text{(photonic: signal + background + cold-shield)},$$

$$NEI_{dar}^2 = NEI_{\det}^2 + NEI_{amp}^2 + NEI_{ro}^2 \qquad \text{(electronic: detector + amplifier + readout)},$$

$$NEI_{sys}^2 = NEI_{xt}^2 + NEI_{dig}^2 + \ldots. \qquad \text{(systematic: cross-talk + digitization + ... + etc.)}.$$

The signal irradiance, also referenced at the detector, is related to the received signal power (at the detector) P_{sig} through

$$I_{sig} = \frac{\lambda_o}{h \cdot c} \cdot \frac{1}{A_d} \cdot P_{sig}$$

where λ_o is the optical center wavelength and A_d is the detectors active optical area. The noise equivalent irradiance of the signal is then given by:

$$NEI_{sig} = \sqrt{\kappa_d \cdot \frac{\Delta f}{\eta_d} \cdot I_{sig}}$$

with Δf the noise equivalent bandwidth (Hz), η_d the detector quantum efficiency and κ_d a scale factor ($\kappa_d = 2$ for a photovoltaic detector). If the transmitted signal is pulsed (pulse width τ_x) and the receiver is temporally windowed (gate width τ_r), the signal to noise ratio becomes

$$SNR_{\det} = \frac{I_{sig} \cdot \tau_x}{\sqrt{NEI_{sig}^2 \cdot \tau_x^2 + \left(NEI_{ph}^2 + NEI_{dar}^2 + NEI_{sys}^2\right) \cdot \tau_r^2}} \qquad \text{[ph-m}^{-2}\text{/ph-m}^{-2} \text{ or e/e]}.$$

where it has been assumed that $\tau_r \geq \tau_x$. Note that the signal noise has been separated from the NEI_{ph} term.
A useful conversion (referenced at the detector) relating noise equivalent irradiance [ph/m2-s] and noise equivalent power is

$$NEI = \frac{\lambda_o}{h \cdot c} \cdot \frac{1}{A_d} \cdot NEP \cdot$$

where λ_o is the optical center wavelength and A_d is the detectors active optical area.

3.1.B. Receiver sensitivity

Once NEI_{tot} is known, the minimum receiver sensitivity (SNR $\approx$ 1) can be estimated with

$$P_{\min} = \frac{h \cdot c}{\lambda_o} \cdot \frac{A_d}{\chi_r \cdot \left(1 - \left(\frac{D_{r\_obs}}{D_r}\right)^2\right)} \cdot NEI_{tot}$$

where P_{min} is the minimum detectable rms power in watts at the receiver aperture, λ_o is the optical center wavelength, A_d is the detectors active optical area, χ_r the receiver optical efficiency, and D_r, D_{r_obs} the receiver aperture diameter and aperture obstruction respectively.

Note that correlated noise (1/f, drift etc.) and white noise are inseparably combined in the NEI terms. Since correlated noise may lead to pathological system behavior, the ability to separate the two is desirable. **Section 4**, *Correlated Noise examines the impact of correlated noise in DIAL systems.*

3.2. Receiver optical efficiency

Receiver optical efficiency is composed of three components: i) optical transmission losses from aperture to detector due to atmosphere and receiver optical losses, ii) optical form factor based on transmitter - receiver configuration and alignment geometry, and iii) energy spreading at the image-plane due to the limitations in optical resolution from target to detector.

3.2.A. Optical transmission efficiency

Optical transmission efficiency from receiver aperture to detector is given by the product of aperture collection efficiency, optical losses and optical filtering losses or

$$Efficiency = \left(1 - \left(\frac{D_{r\_obs}}{D_r}\right)^2\right) \cdot \chi_r \cdot \eta_f ,$$

where D_r, D_{r_obs} are the receiver aperture diameter and aperture obstruction respectively, χ_r the receiver optical efficiency, and η_f the optical filter passband efficiency.

3.2.B. Geometric form factor[3 4 5]

The geometric form factor is the ratio of the fraction of received optical intensity distribution integrated over the detector area to the total transmitted beam optical intensity distribution integral at the target. The intensity distribution, for example a Gaussian beam (TEM_{oo}), is normalized so only the spatial profile is considered. Ideally, the entire transmitted intensity distribution is integrated at the detector leading to a 100% form factor. However, mechanisms including transmitter beam and receiver field-of-view overlap, receiver obstruction (on coaxial systems) and receiver/transmitter separation (on biaxial systems), receiver/transmitter alignment angle, and receiver/target range effectively degrade the form factor. Note that going to a large detector to achieve near 100% form factors may introduce excessive detection noise (see **Section 3.1.**), while a small detector may introduce correlated noise due to detected signal modulation by systematic intensity clipping at the detector.

3.2.C. Optical resolution

Referring to **Figure 5**, the image chain shown is a schematic description of the primary system elements, from target to output, that may lead to the spreading of the spatial intensity distribution at the image plane causing a reduction in detection. The two dimensional transfer function relating input to output can be described either in terms of a *point spread function* (PSF) function or an *optical transfer function* (OTF). The PSF and OTF are Fourier transform pairs (PSF spatial domain x,y [m] $\leftrightarrow$ OTF frequency domain k_x, k_y [cycles/m] or [line-pairs/m]) and represent the linear, optical point source or optical impulse response solution of the image chain system. Since the system is linear, the capture of an arbitrary image, which can be thought of as a continuum of optical point sources, is obtained by the 2-D convolution of the transmitted beam distribution at the target with the PSF or the 2-D product of the Fourier transform of the image and OTF. For a single-spectral line (λ_o), the resulting intensity distribution at the image-plane is given by [6]

Spatial domain: $image_{out} = PSF(\lambda_o) * image_{in}(\lambda_o)$ (spatial domain),

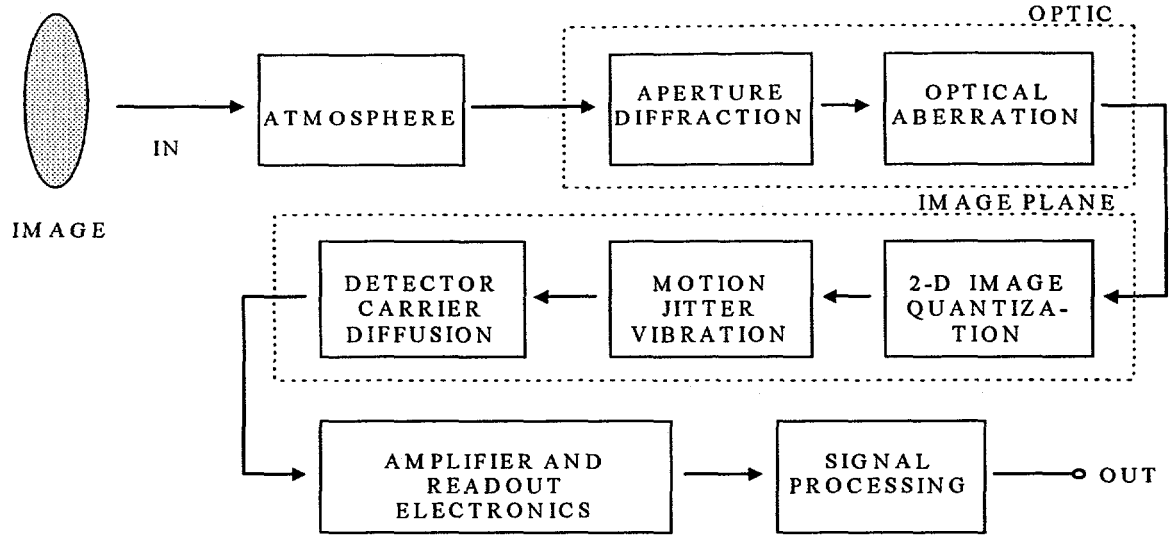

Figure 5. Imaging System.

Frequency domain: $IMAGE_{out} = OTF(\lambda_o) \cdot IMAGE_{in}(\lambda_o)$ (frequency domain),

where:

* = 2-D convolution,

$IMAGE_{in/out}$ = Spatial Fourier Transform ($image_{in/out}$),

$PSF(\lambda)$ = Spatial Inverse Fourier Transform ($OTF(\lambda)$),

$$OTF(\lambda) = OTF_{sp}(\lambda) \cdot OTF_{a/r}(\lambda) \cdot OTF_{cd}(\lambda) \cdot OTF_{rm}(\lambda) \cdot OTF_{2dq}(\lambda) \cdot OTF_{sv}(\lambda) \cdot OTF_{rv}(\lambda) \cdot \ldots$$
$$\ldots \cdot OTF_{ab}(\lambda) \cdot OTF_{ap}(\lambda) \cdot OTF_{atm}(\lambda)$$

The degradation factor due to resolution is defined as the ratio of received "ideal"optical intensity distribution integrated over the detector area to the otf-convolved optical intensity distribution integrated over the detector area. The normalized intensity distribution is the transmitter beam profile at target properly shaped or "clipped" by geometric factors including transmitter/receiver overlap and alignment, and receiver obscuration as described in **Section 3.2.B.**. Note the above OTF terms concerning 2-D quantization, carrier diffusion and amplifier/readout electronic are applicable only to the multi-pixel focal plane array.

4. CORRELATED NOISE

Correlated noise, in a practical sense, is noise whose distinguishing characteristics include a varying power spectral density over the frequency range of interest and conversely, a broadening of it's autocorrelation function (over the temporal range of interest). The primary degrading affect of correlated noise on DIAL is the potential of a reduction in multi-sample averaging efficiencies (non-$\sqrt{n}$ noise convergence). A simplified illustration of the relationship between correlated noise and degradation in averaging efficiencies is shown in Figure 6. If a signal of constant amplitude is detected in the presence of white noise (noise spectral density is flat), the improvement in the standard deviation of the signal-to-noise ratio follows a square root progression when averaged over n-samples. If a signal of constant amplitude is detected in the presence of correlated noise (in this case 1/f and white noise), the improvement in the standard deviation of the signal-to-noise ratio may deviate from the square root progression when averaged over n-samples.

Signal + White Noise

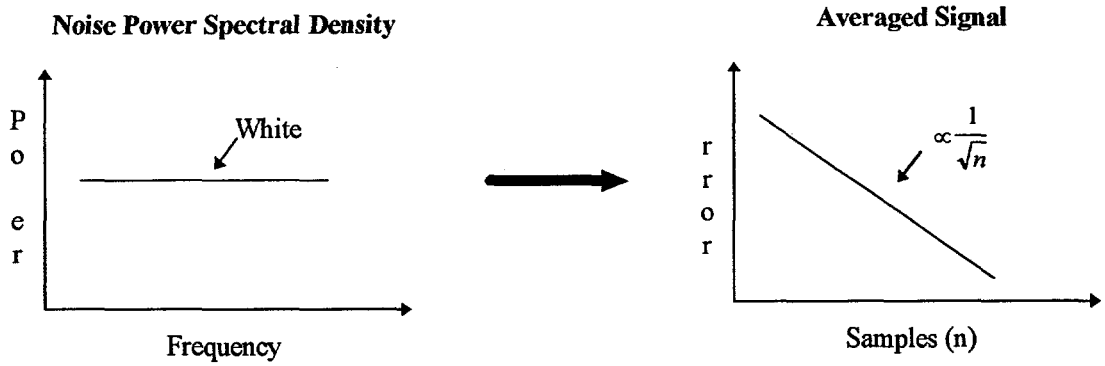

Signal + Correlated Noise

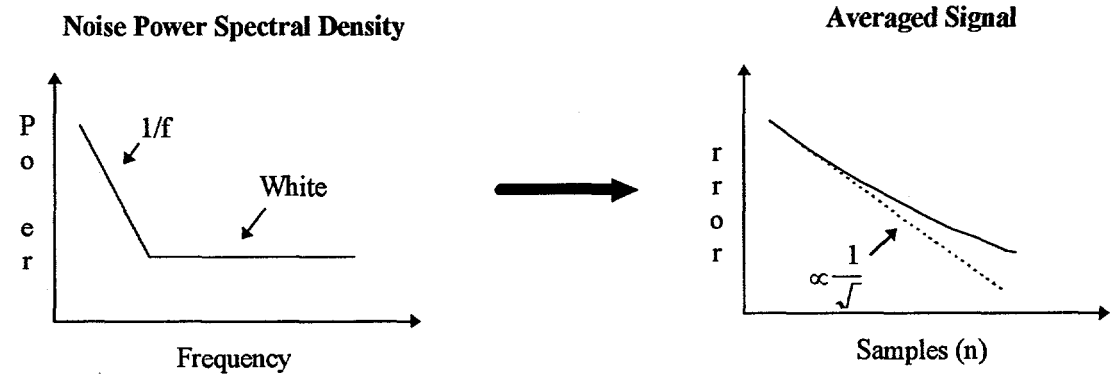

Figure 6. Illustration of Potential Degradation of Multi-Sample Averaged Signal Error Due to Correlated Noise.

4.1. Effects of correlated noise on multi-sample averaging: A numerical example

A numerical simulation of the effects of correlated noise follows. Referring to Figures 7-A through 7-C, a temopral ensemble of 4 noise types x 100 independent traces x 2000 samples per trace were generated. The four types of noise are composed of i) 100 % white noise, ii) 10 % correlated noise and 90 % white noise, iii) 50 % correlated noise and 50 % white noise and iv) 50 % band-limited correlated noise and 50 % white noise. By a bounded noise spectrum, we mean that the correlated noise returns to the white noise floor within the noise trace power spectral density. Each noise trace has a zero mean with a standard deviation = 0.9 with the correlated source composed of 1/f noise (see Figure 7-A for example traces). The corresponding ensemble averaged autocorrelations are plotted in Figures 7-B, and the ensemble averaged multi-sample error reduction is shown in Figure 7-C. The following observations are worth emphasizing:

- White noise, as expected, produces a $\sqrt{n}$ reduction in the standard deviation when averaged over n samples.
- Correlated noise increases the number of averaged samples required to achieve a desired level of error.
- The magnitude of degradation (relative to $\sqrt{n}$ reduction efficiencies) due to correlated noise depends on the amount of correlated noise present, its spectral content relative to the sampled signal and whether the noise spectrum is bounded (compare the 50% band-limited noise case with the 50% unbound case).

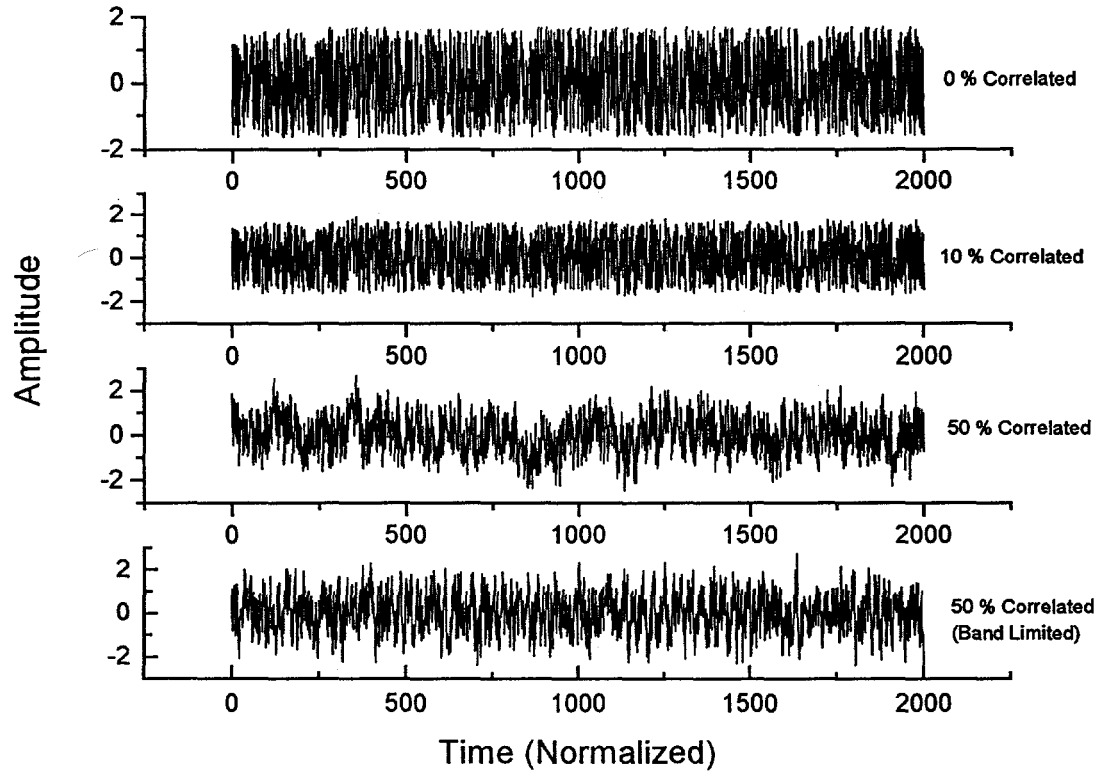

Figure 7-A. Example Noise Traces (Ensemble Size = 100 Traces).

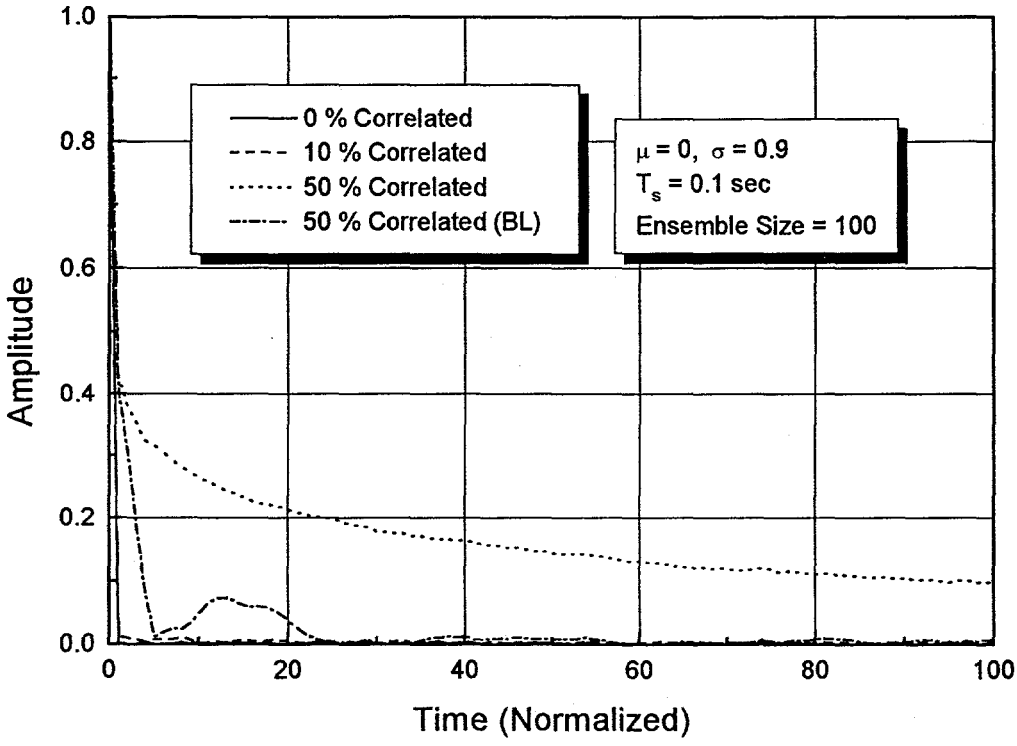

Figure 7-B. Ensemble Averaged Autocorrelation.

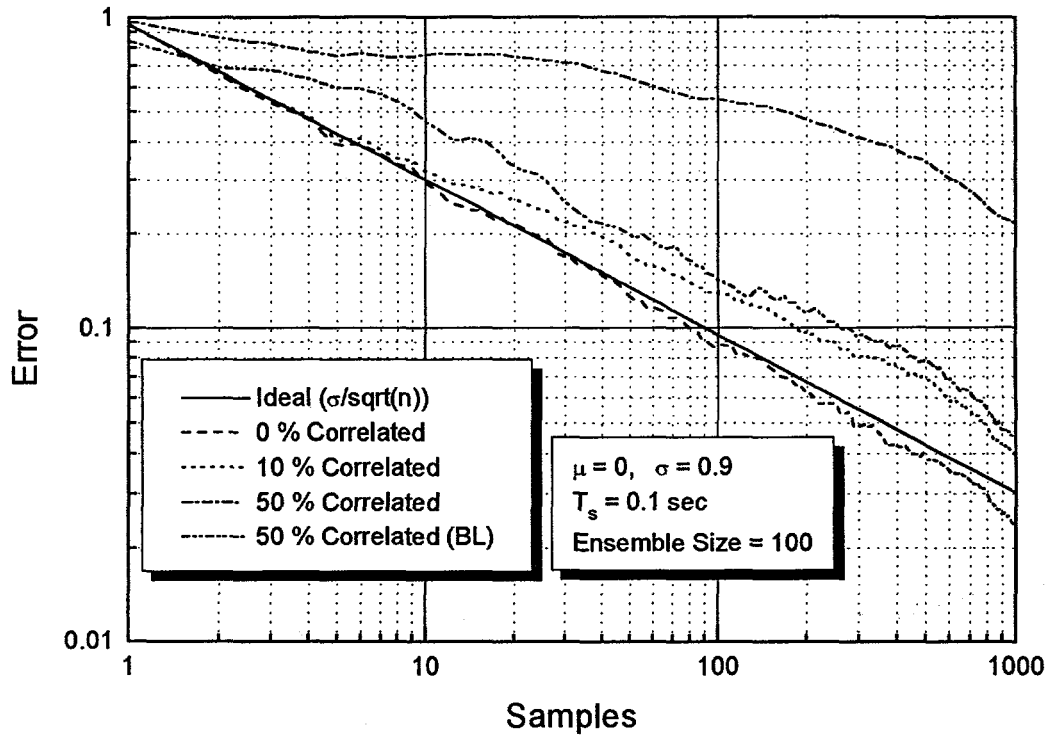

Figure 7-C. Ensemble Averaged Error Reduction Through Sample Averaging.

4.2. Sources of correlated noise

The typical sources of correlated noise in DIAL include non-random fluctuations in transmitter (temporal, spectral and spatial), receiver (detector and electronics)[7 8], transmitter/receiver geometric form factor fluctuations, atmosphere[9] and target statistics[10 11] (speckle, albedo and plume dynamics). The most commonly encountered, and most widely studied, correlated noise is one-over-frequency noise. Low-frequency one-over-frequency (1/f) noise is a class of noise that is widespread in nature and whose noise spectral density follows a $1/f^{\beta}$ distribution (typically $0 \le \beta \le 2$)[12 13]. By studying the sources and nature of correlated noise, efforts are underway to develop techniques and algorithms to mitigate its potentially degrading effects on DIAL.

5. PROTOTYPE LOW-NOISE, WHITE RECEIVER DETECTION SYSTEM

Based on our current understanding of receiver/transmitter noise physics, we are in the processes of developing low noise, "white" receiver systems whose averaged output follow a $\sqrt{n}$ progression. Figure 8 shows a prototype system. The receiver is based on a low-noise transimpedance amplifier with active baseline restoration for 1/f noise reduction. It implements a pseudo matched-filter or correlated detection system with peak detection and time-of-flight discriminator. The shaping filter h(t) is selected to maximize the detection signal to noise ratio seen at the peak detector. The signal to noise ratio

$$SNR = \frac{s(t) * h(t)}{\sqrt{n(t) * h(t)}},$$

is maximized when the matched filter[14] requirement $h(t) = s^*(t)$ is satisfied. Correlated detection, which is easier to implement than a matched filter, occurs for $h(t) \approx s(t)$.

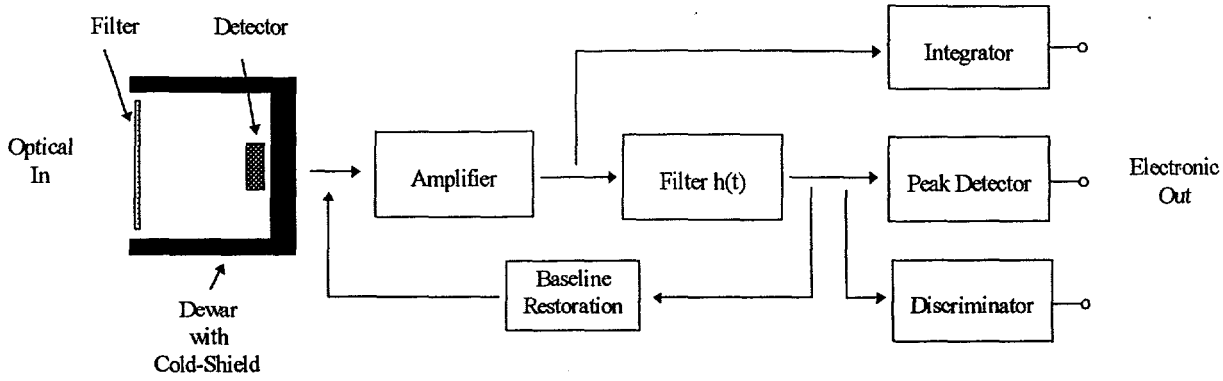

Figure 8. Prototype Receiver Detection System.

The prototype was designed to detect return pulses from a high-repetition-rate, 100 ns pulse-width laser. The 5th order shaping filter is designed with a 100 ns full-width, half-maximum (FWHM) for optimal pulse detection. A 100-200 μm, λ_c = 11 μm $Hg_{1-x}Cd_xTe$ photovoltaic, that will be cooled below 77 K to match the amplifiers noise floor, will be the principle detector. A summary of the amplifier and detector effort are summarized in **Sections 5.1.** and **5.2.** respectively.

5.1. Transimpedance amplifier measurement summary:

Nominal experimental configuration (unless otherwise stated): Uncooled amplifier with ambient temperature ~ 75° F, 500 kΩ / 10 pF source impedance (projected 100 - 200 μm detector @ 50 K), 1 kΩ load impedance, 10 kHz pulse repetition rate (PRR), and ± 5 V supply.

- Amplifier Topology: Transimpedance.
- Gain: 10^6 V/A into 1 kΩ load, $5 \cdot 10^5$ V/A into 50 Ω load.
- Shaping Filter: 100 ns full-width, half maximum (FWHM).
- DC Baseline Drift: Less than ± 100 μV.
- 1/f Correlated Noise Rejection: DC to 5 kHz, spectral magnitude lost in white noise floor.
- White Noise Floor: 300 - 400 fA/√Hz.
- Total Noise: I_n = 2 - 2.5 nA (rms) or NEP ~ 250 pW (referenced @ λ = 10.6 μm).
- Noise Bandwidth: 10 to 20 MHz depending on excess noise (due to detector capacitance).
- Linear Dynamic Range: Greater than 1000:1 (ideal for 12 - bit ADC).
- Maximum PRR: 1 MHz with 100 ns pulse.

Noise spectral density and amplifier impulse response are shown in **Figures 9.A** and **9.B** respectively.

5.2. Detector

The targeted detector is a 100-200 μm, $Hg_{1-x}Cd_xTe$ (λ_c = 11 μm) photovoltaic. In order to match the amplifier noise floor, the detector's electro-optic specifications require quantum efficiency: ≥ 60 %, dark current @ -50 mV bias: ≤ 0.5 μA, dynamic impedance @ -50 mV bias: ≥ 500 kΩ, capacitance @ -50 mV bias: ~ 10-20 pF. These numbers are currently unachievable at LN_2 temperatures and we are investigating the prospects of cooling the detector below 77 K. **Table 1.** tabulates RoA vs temperature over the range of 25 K to 77 K for a 100 μm, $Hg_{1-x}Cd_xTe$ (λ_c = 11 μm) photovoltaic. The tabulated RoA values, which are a first order measure of the detectors noise performance, deviate from calculations and are far lower than theory predicts. In addition, at reverse bias levels greater than 5 - 10 mV,

Temperature [K]	RoA [Ω-cm^2]
77	0.28
75	0.35
70	0.61
65	1.20
60	1.95
55	2.66
50	3.58
45	4.83
35	9.24
25	12.75

Table 1. Detector RoA vs Temperature.

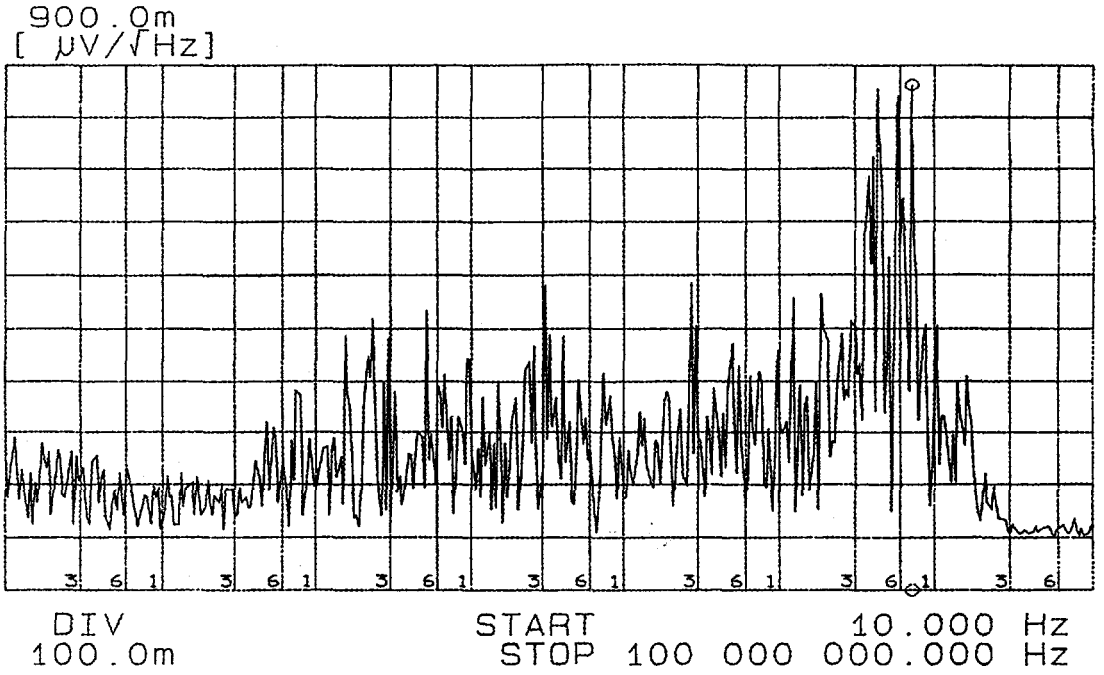

Figure 9.A. Noise Spectral Density (Hewlett Packard 4195A).

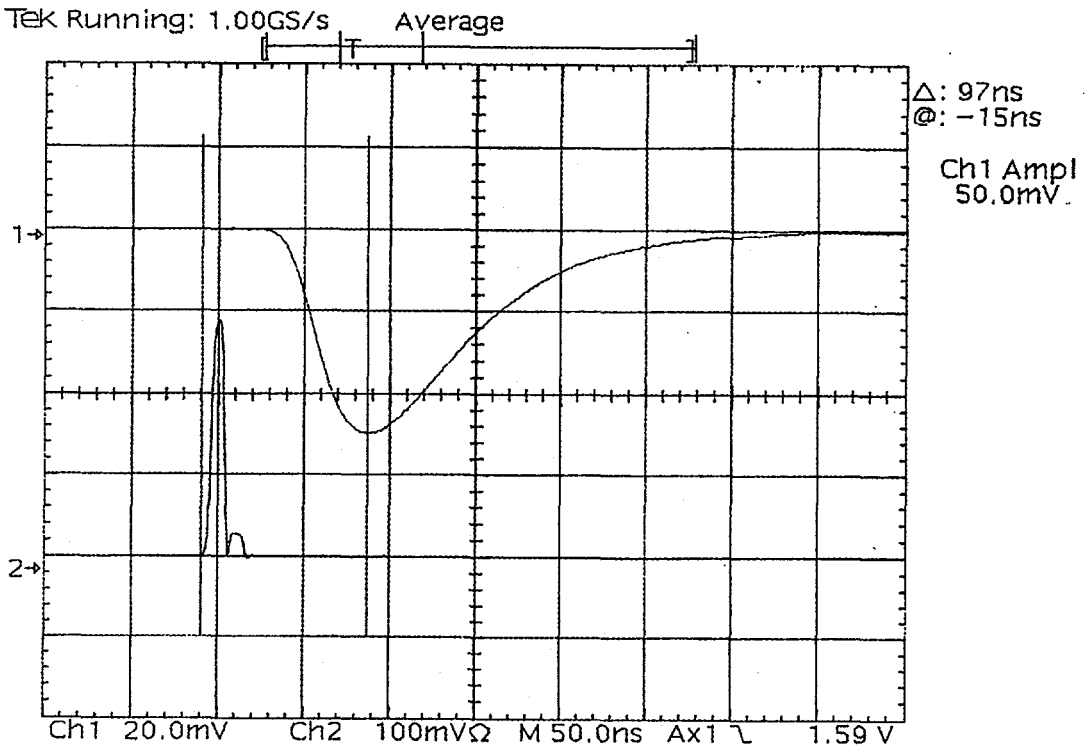

Figure 9.B. Amplifier Impulse Response (Tektronix TDS 620).

dark currents are on the same order of magnitude. For reasons of fairness (their detector is designed for 77 K operation), the detector vendor shall remain unnamed. We believe the inability to achieve predicted values of RoA is due to surface effects. It has been reported in the literature[15] that the manufacturing capabilities are available to develop detectors with RoA values that approach theoretical limits at temperatures below 77 K. These measurements were carried out in a temperature controlled helium dewar with a low 77 K blackbody background[16].

6. CONCLUSION

We have provided a general overview of our DIAL transmitter/receiver system noise characterization efforts and a numerical simulation demonstrating that correlated noise may increase the number of averaged samples required to achieve a desired level of error. Based on our current understanding of the of receiver/transmitter noise processes, we have proposed a low noise, protoype receiver system. We have designed and built a low-noise amplifier with a suppressed 1/f noise component, and we are carrying out experiments on detector noise reductions.

7. ACKNOWLEDGMENTS

The submitted manuscript has been authored by an employees of the University of California, operator of the Los Alamos National Laboratory under Contract No. W-7405-ENG-36 with the U.S. Department of Energy. Accordingly, the U.S. Government retains an irrevocable, nonexclusive, royalty-free license to publish, translate, reproduce, use, or dispose of the published form of the work and to authorize others to do the same for U.S. Government purposes.

8. REFERENCES

[1] A. Papoulis, *Probability, Random Variables and Stochastic Processes*, McGraw-Hill, City, 1984.

[2] J. Vampola, *Readout Electronics For Infrared Sensors, The IR Electro-Optical Systems Handbook*, Vol. 3, SPIE Press, City 1993.

[3] J. Harms, "Lidar return signals for coaxial and noncoaxial systems with central obstructions," *Applied Optics*, Vol. 18(10), pp. 1559-1566, May 1979.

[4] T. Halldorsson, and J. Langerholc, "Geometrical for factors for the lidar function," *Applied Optics*, Vol. 17(2), pp. 240-244, January 1978.

[5] J. Harms, W. Lahmann, and C. Weitkamp, "Geometrical compression of lidar return signals," *Applied Optics*, Vol. 17(7), pp. 1131-1135, April 1978.

[6] J. W. Goodman, *Introduction to Fourier Optics*, McGraw-Hill, City, 1968.

[7] Special issue on fluctuation phenomena in electronic and photonic devices, *IEEE Trans. Elect. Dev.*, Vol. 41(11), pp. 1889-2222, November 1994.

[8] S. Czuchlewski, et. al., "Signal-to-noise issues and detector optimization for 10 μm CO_2 DIAL," CALIOPE Interim Technical Review, March 1995.

[9] N. Menyuk, D. K. Killinger, and C. R. Menyuk, "Error reduction in laser remote sensing: Combined effects of cross correlation and signal averaging," *Applied Optics*, Vol. 24(1), January 1985.

[10] M. Schmitt, et. al., "A comprehensive model for CO_2 DIAL: An overview," CALIOPE Interim Technical Review, March 1995.

[11] E. Mackerrow, et. al., "Field measurement of speckle effects on CO_2 DIAL," CALIOPE Interim Technical Review, March 1995.

[12] M. S. Keshner, "1/f noise," *Proc. of the IEEE*, Vol. 70(3), pp. 212-218, March 1982.

[13] F. N. Hooge, "1/f noise," *Physica*, Vol. 83B, pp. 14-23, 1976.

[14] J. Minkoff, *Signals, Noise, & Active Sensors*, John Wiley & Sons, City, 1985.

[15] G. Destefanis and J. P. Chamonal, "Large Improvement in HgCdTe Photovoltaic Detector Performances at LETI," *J. Electronic Materials*, Vol. 22(8), pp. 1027-1032, 1993.

[16] K. M. Hays, D. L. Rawlins, M. D. Petroff, and M. G. Stapelbroek, "Ultra-Low Background Dewar for Infrared Detector Characterization Studies," *SPIE Test and Evaluation of Infrared Detectors and Arrays*, Vol. 1108, pp. 77-83, 1989.